Volume 1 | Number 1 | Jan 2013 | Pages 1–100

Dalton Transactions

An international journal of inorganic chemistry
www.rsc.org/dalton

ROYAL SOCIETY OF CHEMISTRY

ROYAL SOCIETY OF CHEMISTRY

www.rsc.org/dalton

Journal Name

ARTICLE

Microwave-assisted large scale synthesis of lanthanide Metal− Organic Frameworks (Ln-MOFs), having preferred conformation and photoluminescence properties

Partha Pratim Bag, Xu-Sheng Wang and Rong Cao*

Preparation of MOF in large scale is a great challenge due to difficulties in reproducibility. Microwave synthesis procedure acts a major role to solve this problem. Moreover, preferred conformation achievement, in case of flexible ligand is also an important factor as it belongs to stability of MOF. In this regard, lanthanides are suitable candidate due to their large size and coordination capability. A series of isostructural microporous lanthanide metal−organic frameworks (Ln-MOFs), formulated as [Ln (TTTPC)(NO$_2$)$_2$(Cl)]·(H$_2$O)$_{10}$ {Ln = La (**1**), Ce (**2**), Pr (**3**), Nd (**4**), Eu (**5**), Tb (**6**), Dy (**7**), Ho (**8**), Yb (**9**); H$_3$TTTPC = 1,1',1"-tris(2,4,6-trimethylbenzene-1,3,5- triyl)-tris(methylene)-tris(pyridine-4-carboxylic acid)}, has been synthesized in large scale under microwave-assisted solvothermal reaction for 5 min. Otherwise, if a conventional solvothermal reaction is carried out under the same temperature, a much longer time (2 days) and from slow evaporation 5 days are needed for the same phase in similar yield. Moreover, in this circumstance conventional methods are useful only for small scale (10 mg) synthesis, but using MWASR up to 2 g was obtained. Structure analysis reveals that the framework of the as-synthesized MOFs is a 6-connected network with point symbol (4^11.6^4), which is a subnet of uninodal net having new topology sqc885. Thermal gravimetric analyses performed on as-synthesized MOFs reveal that the frameworks have moderate thermal stability. Gas sorption properties of **1** and **8** were studied by experimentally measuring nitrogen and hydrogen sorption isotherms. The luminescent properties of **5** and **6** were investigated and show characteristic emissions for Eu^{3+} and Tb^{3+} at room temperature.

Introduction

In the last few years, research on metal−organic frameworks (MOFs) reveals that are important class of porous materials and have been widely explored because of their fascinating structures[1] and their potential applications in gas adsorption and separation, magnetism, catalysis, molecular recognition etc.[2] Compared to MOFs based on first-row transition metal ions, lanthanide ions have larger coordination spheres favor the formation of densely packed structures[3] and more flexible coordination geometries resulting less porous materials. So far, many searches for reported Ln-MOFs have focused on magnetic and photo luminescent properties;[4] it is still challenging to construct porous Ln-MOFs with flexible ligand to scale up having maximum purity due to its flexibility.

So far, metal−organic frameworks are predominantly synthesized under hydrothermal/solvothermal condition which requires long reaction times (days to weeks) and heavy energy consumption and sometimes scale up of typical batch processes can lead to unsuccessful or low quality synthesis for some systems. So, it is a challenging task to develop a facile, rapid, and economical route for the syntheses of pure MOFs in large scale for practical applications. Generally, simple and energy-efficient heating process, microwave synthesis can dramatically reduce the reaction time and enhance product yields. This method has been frequently used in organic synthesis[5] and in the preparation of nanoporous inorganic materials.[6] But very recently, this method has also been applied to prepare metal clusters[7] and MOFs with known structures.[8] Recently we have shown the synthetic ability of MOF using microwave.[9] After getting inspiration from this result, now we synthesized pure MOF in large scale. But unfortunately, due to fast kinetics of crystal nucleation and growth, only micro sized crystals of MOFs are often prepared by this method. Although some novel coordination polymers were prepared by microwave method through careful design of the synthetic conditions,[10] the

application of microwave method in the large scale preparation of pure MOFs is still limited.

The synthesis of MOF using rigid ligand is easier than the flexible one, so former are more cultivated and these are well described in the review of Zhou.[11] It is more difficult to construct MOFs with flexible ligand due to the flexibility and so the ligand itself can adopt different conformations and thus lead to distinct symmetries during the self-assembly process. The structures of flexible MOFs are more dependent on the reaction parameters including temperature, time, pH etc.[12] These factors severely obstruct the development of knowledge and concepts for the rational design and prediction of extended network architectures with flexible organic ligands.[13] Most of the flexible MOFs are turn fragile and may lose their porosities after removal of guest molecules because of the ligand flexibility that can collapse the skeleton of frameworks.

Herein, we report the microwave-assisted solvothermal scale up synthesis of a series of isostructural three-dimensional (3D) lanthanide MOFs (Ln-MOFs) with luminescence and gas adsorption properties, formulated as [Ln(TTTPC)(NO$_2$)$_2$(Cl)]·(H$_2$O)$_{10}$ {Ln = La (**1**), Ce (**2**), Pr (**3**), Nd (**4**), Eu (**5**), Tb (**6**), Dy (**7**), Ho (**8**), Yb (**9**); H$_3$TTTPC = 1,1',1"-tris(2,4,6-trimethylbenzene-1,3,5-triyl)-tris(methylene)-tris(pyridine-4-carboxylic acid)}. The flexible ligand may exist in different conformations. Here we showed that most preferable conformation *i.e.*, less energetic form of this ligand is adopted by all the lanthanides, which support the theoretical calculation but contradict to the previous report.[26] We present the syntheses and detailed structure descriptions of nine isostructural Ln-MOFs along with the topology studies. Besides, we have studied the solid-state emission spectra of **5** and **6**. Furthermore, we also illustrated the pore characteristics and gas sorption properties of **1** and **8** by experimentally measuring nitrogen and hydrogen sorption isotherms where selectively hydrogen adsorptions occur preferably due to narrow pore size of MOFs.

Experimental

General remarks

All chemicals, ligand H$_3$TTTPC and solvent purchased were of reagent grade and used without further purification. Microwave assisted solvothermal syntheses were carried out in a microwave oven (Initiator 8 EXP, 2450 MHz frequency, Biotage Corp.). Elemental analyses (C, H, and N) were carried out on an Elementar Vario EL III analyzer. Powder X-ray diffraction (PXRD) data were collected on a Rigaku MiniFlex2 diffractometer working with Cu Kα radiation, and the recording speed was 5° min^{-1} over the 2θ range of 5 − 50° at room temperature. Thermogravimetric analyses (TGA) were recorded on a NETZSCH STA 449C unit at a heating rate of 10 °C min^{-1} under flowing nitrogen atmosphere. ^{1}H NMR spectra were recorded at ambient temperature on a Bruker Avance III spectrometer; the chemical shifts were referenced to TMS in the solvent signal in d_6-DMSO. Fluorescence spectroscopy data were recorded on a FLS920 fluorescence spectrophotometer. The Scanning Electron Microscopy (SEM) images are taken on JEOL JSM-6700F instrument. The simulated powder patterns were calculated using Mercury 2.0. The purity and homogeneity of the bulk products were determined by comparison of the simulated and experimental X-ray powder diffraction patterns. The images of crystals were captured using Canon EOS 60D digital camera under the microscope CEWEI PXS5-B1.

Synthesis of [La(TTTPC)(O)$_2$(NO$_2$)$_2$(Cl)]•(H$_2$O)$_{10}$ (1). La(NO$_3$)$_3$·6H$_2$O (0.0471 mmol, 20.45 mg), H$_3$TTTPC (0.0157 mmol, 10 mg), a mixed solvent (1 mL, H$_2$O/EtOH = 1:1) were placed together in a 2 mL microwave tube. The mixture was heated by microwave under autogenous pressure at 85 °C for 5 min, and then cooled naturally to room temperature. The compound can also be synthesized by a conventional solvothermal reaction at the same temperature for 2 days for the same phase in similar yield. Colorless crystals suitable for single-crystal X-ray diffraction were obtained by filtration, washed for several times with H$_2$O/EtOH (1:1), and dried in air at ambient temperature. The compound is stable in air and insoluble in common organic solvents such as methanol, ethanol, acetonitrile, acetone, dimethylsulfoxide, and DMF. Yield: 75% (based on H$_3$TTTPC). Anal. Calcd for C$_{30}$H$_{47}$LaClN$_5$O$_{24}$ (Mr = 1036.07): C, 34.78; H, 4.57; N, 6.76. Found: C, 34.94; H, 4.76; N, 6.85. IR (KBr pellet, ν/cm^{-1}): 1607(s), 1564(s), 1412(m), 1383(s), 1348(m), 1211(w), 1131(m), 1044(m), 873(w), 796(w), 772(w), 734(w), 692(m), 636(w), 594(w), 552(w), 510(w).

Synthesis of [Ce(TTTPC)(O)$_2$(NO$_2$)$_2$(Cl)]•(H$_2$O)$_{10}$ (2). The colorless crystals were prepared similarly from Ce(NO$_3$)$_3$·6H$_2$O.Yield: 80% (based on H$_3$TTTPC). Anal. Calcd for C$_{30}$H$_{47}$CeClN$_5$O$_{24}$ (Mr = 1037.28): C, 34.74; H, 4.57; N, 6.75. Found: C, 34.39; H, 4.42; N, 7.10. IR (KBr pellet, ν/cm^{-1}): 1614(s), 1564(s), 1411(m), 1383(s), 1348(w), 1201(w), 1138(m), 1041(m), 873(w), 825(w), 803(w), 772(m), 727(w), 699(m), 629(w), 553(w), 517(w).

Synthesis of [Pr(TTTPC)(O)$_2$(NO$_2$)$_2$(Cl)]•(H$_2$O)$_{10}$ (3). The colorless crystals were prepared similarly from Pr(NO$_3$)$_3$·6H$_2$O. Yield: 70% (based on H$_3$TTTPC). Anal. Calcd for C$_{30}$H$_{47}$PrClN$_5$O$_{24}$ (Mr = 1038.07): C, 34.71; H, 4.56; N, 6.75. Found: C, 34.74; H, 4.36; N, 7.15. IR (KBr pellet, ν/cm^{-1}): 1621(s), 1557(s), 1411(m), 1250(w), 1198(w), 1138(m), 1041(m), 880(m), 796(w), 769(m), 730(m), 699(w), 664(w), 636(w), 559(w), 517(w).

Synthesis of [Nd(TTTPC)(O)$_2$(NO$_2$)$_2$(Cl)]•(H$_2$O)$_{10}$ (4). The colorless crystals were prepared similarly from Nd(NO$_3$)$_3$·6H$_2$O. Yield: 75% (based on H$_3$TTTPC). Anal. Calcd for C$_{30}$H$_{47}$NdClN$_5$O$_{24}$ (Mr = 1041.41): C, 34.71; H, 4.56; N, 6.75. Found: C, 34.78; H, 4.41; N, 7.85. IR (KBr pellet, ν/cm^{-1}): 1610(s), 1567(s), 1411(m), 1383(s), 1207(w), 1139(m), 1041(m), 873(w), 803(w), 769(w), 727(w), 692(m), 636(w), 559(w), 517(w).

Synthesis of [Eu(TTTPC)(O)$_2$(NO$_2$)$_2$(Cl)]•(H$_2$O)$_{10}$ (5). The colorless crystals were prepared similarly from

Eu(NO$_3$)$_3$·6H$_2$O. Yield: 80% (based on H$_3$TTTPC). Anal. Calcd for C$_{30}$H$_{47}$EuClN$_5$O$_{24}$ (Mr = 1049.13): C, 34.34; H, 4.52; N, 6.68. Found: C, 34.44; H, 4.51; N, 6.65. IR (KBr pellet, ν/cm^{-1}): 1620(s), 1557(s), 1417(m), 1389(s), 1352(w), 1212(w), 1130(m), 1049(m), 878(w), 835(w), 800(w), 777(m), 721(w), 692(m), 623(w), 560(w), 520(w).

Synthesis of [Tb(TTTPC)(O)$_2$(NO$_2$)$_2$(Cl)]•(H$_2$O)$_{10}$ (6). The colorless crystals were prepared similarly from Tb(NO$_3$)$_3$·6H$_2$O. Yield: 65% (based on H$_3$TTTPC). Anal. Calcd for C$_{30}$H$_{47}$TbClN$_5$O$_{24}$ (Mr = 1056.09): C, 34.12; H, 4.49; N, 6.63. Found: C, 34.52; H, 4.55; N, 6.75. IR (KBr pellet, ν/cm^{-1}): 1612(s), 1559(s), 1420(m), 1389(s), 1139(m), 1048(m), 875(w), 788(w), 780(w), 730(w), 700(m), 642(w), 600(w), 562(w), 512(w).

Synthesis of [Dy(TTTPC)(O)$_2$(NO$_2$)$_2$(Cl)]•(H$_2$O)$_{10}$ (7). The colorless crystals were prepared similarly from Dy(NO$_3$)$_3$·6H$_2$O. Yield: 70% (based on H$_3$TTTPC). Anal. Calcd for C$_{30}$H$_{47}$DyClN$_5$O$_{24}$ (Mr = 1059.67): C, 34.00; H, 4.47; N, 6.61. Found: C, 34.30; H, 4.50; N, 6.73. IR (KBr pellet, ν/cm^{-1}): 1614(s), 1553(s), 1419(m), 1389(s), 1342(w), 1210(w), 1132(m), 1047(m), 879(w), 832(w), 800(w), 764(m), 720(w), 690(m), 625(w), 558(w), 513(w).

Synthesis of [Ho(TTTPC)(O)$_2$(NO$_2$)$_2$(Cl)]•(H$_2$O)$_{10}$ (8). The colorless crystals were prepared similarly from Ho(NO$_3$)$_3$·6H$_2$O. Yield: 75% (based on H$_3$TTTPC). Anal. Calcd for C$_{30}$H$_{47}$HoClN$_5$O$_{24}$ (Mr = 1062.10): C, 33.93; H, 4.46; N, 6.59. Found: C, 34.14; H, 4.66; N, 6.75. IR (KBr pellet, ν/cm^{-1}): 1607(s), 1570(s), 1417(m), 1385(s), 1219(w), 1137(m), 1050(m), 880(w), 791(w), 764(w), 739(w), 685(m), 629(w), 599(w), 546(w), 509(w).

Synthesis of [Yb(TTTPC)(O)$_2$(NO$_2$)$_2$(Cl)]•(H$_2$O)$_{10}$ (9). The colorless crystals were prepared similarly from Yb(NO$_3$)$_3$·6H$_2$O. Yield: 70% (based on H$_3$TTTPC). Anal. Calcd for C$_{30}$H$_{47}$YbClN$_5$O$_{24}$ (Mr = 1070.21): C, 33.67; H, 4.43; N, 6.54. Found: C, 34.02; H, 4.56; N, 6.69. IR (KBr pellet, ν/cm^{-1}): 1614(s), 1572(s), 1420(m), 1373(s), 1355(w), 1220(w), 1144(m), 1048(m), 868(w), 832(w), 799(w), 767(m), 737(w), 691(m), 623(w), 560(w), 517(w).

Table 1. Crystal data^a and structure refinement of 1−4

	1-La	**2**-Ce	**3**-Pr	**4**-Nd
Chemical formula	C$_{30}$H$_{27}$Cl N$_5$O$_{14}$La	C$_{30}$H$_{27}$Cl N$_5$O$_{14}$Ce	C$_{30}$H$_{27}$Cl N$_5$O$_{14}$Pr	C$_{30}$H$_{27}$Cl N$_5$O$_{14}$Nd
Formula weight	855.93	857.14	857.93	861.26
Cryst syst	triclinic	triclinic	triclinic	triclinic
Space group	P-1	P-1	P-1	P-1
a/Å	9.55740(10)	9.5251(3)	9.5300(3)	9.52970(10)
b/Å	12.6056(2)	12.5605(4)	12.5401(4)	12.6996(3)
c/Å	18.9892(3)	18.9231(6)	18.8719(6)	18.8203(3)
$α$/deg	106.1310(10)	106.077(3)	105.932(3)	106.347(2)
$β$/deg	98.9710(10)	98.874(3)	98.860(2)	98.6300(10)
$γ$/deg	100.4790(10)	100.643(3)	100.482(2)	100.059(2)
Volume/Å^3	2108.78(5)	2086.80(11)	2082.30(11)	2103.64(6)
D_{calcd} /g cm^{-3}	1.384	1.364	1.368	1.360
$μ$/mm^{-1}	1.137	9.563	10.111	1.359
$θ$ range /°	3.10−29.04	3.76−73.54	3.80−73.14	3.09−28.06
Z	2	2	2	2
Range h	-13— +12	-11— +11	-11— +10	-12— +11
Range k	-16— +16	-15— +14	-15— +15	-15— +16
Range l	-22— +25	-23— +23	-23— +23	-24— +24
Reflns collected	28175	15762	15822	20573
Independent reflns	10138	8067	8023	8882
Obsd reflns	8730	7472	7213	7985
T (K)	100	100	100	100
R_1^{b}	0.0596	0.0582	0.0559	0.0634
wR_2^{c}	0.1769	0.1652	0.1593	0.1799
GOF	1.083	1.074	1.083	1.093
CCDC no.	1052999	1053000	1053001	1053002

^{a}Obtained with graphite-monochromated Mo K$α$ ($λ$ = 0.710 73 Å) and Cu K$α$ ($λ$ = 1.54184 Å) radiation according to requirement. ^{b}R$_1$ = Σ ‖F$_o$| − |Fc ‖/Σ|Fo|. ^{c}wR2 = {Σ[w(Fo2 − Fc2)2]/Σ[w(Fo2)2]}$^{1/2}$.

Table 2. Crystal data^a and structure refinement of 5−9

	5-Eu	**6**-Tb	**7**-Dy	**8**-Ho	**9**-Yb
Chemical formula	$C_{30}H_{27}ClN_5O_{14}Eu$	$C_{30}H_{27}ClN_5O_{14}Tb$	$C_{30}H_{27}ClN_5O_{14}Dy$	$C_{30}H_{27}ClN_5O_{14}Ho$	$C_{30}H_{27}ClN_5O_{14}Yb$
Formula weight	868.98	875.94	879.52	881.95	890.06
Cryst syst	triclinic	triclinic	triclinic	triclinic	triclinic
Space group	P-1	P-1	P-1	P-1	P-1
a/Å	9.4977(3)	9.53070(10)	9.4727(2)	9.4644(2)	9.4951(3)
b/Å	12.6270(4)	12.7016(3)	12.6520(4)	12.7206(3)	12.5595(4)
c/Å	18.7072(4)	18.8199(3)	18.6017(6)	18.5539(5)	18.9191(6)
α/deg	106.096(2)	106.349(2)	106.106(3)	106.206(2)	106.107(3)
β/deg	98.452(2)	98.6290(10)	98.088(2)	97.893(2)	98.869(2)
γ/deg	100.275(2)	100.060(2)	100.255(2)	100.266(2)	100.650(3)
Volume/Å^3	2074.70(10)	2104.13(6)	2064.63(10)	2068.88(9)	2079.23(11)
D_{calcd} /g cm^{-3}	1.391	1.383	1.415	1.416	1.422
μ/mm^{-1}	11.961	1.806	10.828	4.715	5.298
θ range /°	3.71−73.52	4.80−73.44	4.82−73.52	4.82−73.53	3.74−73.56
Z	2	2	2	2	2
Range h	-11— +11	-12— +12	-8— +11	-11— +7	-11— +11
Range k	-15— +15	-15— +16	-15— +15	-15— +15	-15— +14
Range l	-15— +22	-24— +23	-23— +20	-22— +23	-23— +23
Reflns collected	15562	20569	15375	13861	10762
Independent reflns	8035	8879	8016	8012	7962
Obsd reflns	7542	7977	7584	7675	6872
T (K)	100	100	100	100	100
R_1^b	0.0847	0.0622	0.0714	0.0783	0.0632
$wR2^c$	0.2217	0.1771	0.1930	0.2181	0.1816
GOF	1.029	1.091	1.062	1.055	1.064
CCDC no.	1053003	1053004	1053005	1053006	1053007

^{a}Obtained with graphite-monochromated Mo Kα (λ = 0.710 73 Å) and Cu Kα (λ = 1.54184 Å) radiation according to requirement. ^{b}R$_1$ = $\Sigma \| F_o| - |Fc \|/\Sigma|Fo|$.
^{c}wR2 = $\{\Sigma[w(Fo2 - Fc2)2]/\Sigma[w(Fo2)2]\}^{1/2}$.

Single-crystal X-ray crystallography

Single-crystal X-ray diffraction data of all the compounds were collected on a SuperNova, Dual, Cu at zero, Atlas diffractometer. The crystals were kept at 100(16) K during data collection. The structures were solved with the SHELXS[14] structure solution program using Direct Methods and refined with the SHELXL[15] refinement package using Least Squares minimisation. All non-hydrogen atoms were refined with anisotropic displacement parameters. The positions of hydrogen atoms attached to carbon atoms were generated geometrically. Attempts to locate and model the disordered solvent molecules in the pores were unsuccessful. So, we employed PLATON/SQUEEZE[16] to calculate the contribution to the diffraction from the solvent region and thereby produced a set of solvent-free diffraction intensities. The coordinated H$_2$O in this structure are determined according to charge balance and a rational experimental bond and angle parameters which is well consistent with the experiment data ever reported.[17] The final formula was calculated from the SQUEEZE results combined with elemental analysis data and TGA data. Crystallographic data and structure refinement parameters for this crystal are summarized in Table 1 and 2. Selected bond lengths and angles for **1**−**9** were listed in Tables S1−S9 in the Supporting Information. More details on the crystallographic studies as well as atomic displacement parameters are given in Supporting Information as CIF files. Crystallographic data for the structures reported in this paper has been deposited. The following crystal structure has been deposited at the Cambridge Crystallographic Data Centre and allocated the deposition number (CCDC No. 1052999−1053007) for compounds **1**−**9**. These data can be obtained free of charge *via* www.ccdc.cam.ac.uk/data_request/ cif.

Gas adsorption measurements

Low-pressure gas adsorption measurements were carried out on an ASAP (accelerated surface area and porosimetry) 2020 system. The desolvated samples were prepared as follows: A fresh sample was soaked in methanol for 24 h, and the extract was discarded. Fresh methanol was subsequently added, and the

sample was allowed to soak for another 24 h to remove H_2O solvates. The sample was then treated with dichloromethane in the same procedures to remove methanol solvates; after the removal of dichloromethane by decanting, the sample was activated by supercritical carbon dioxide (SCD) method.[18] Supercritical CO_2 drying processes was performed using a Tousimis[TM] Samdri® PVT-30 critical point dryer (Tousimis Rockvill, MD, USA). Before gas adsorption measurement, the sample was dried again by using the "outgas" function of the surface area analyzer for 8 h at 353 K. The measurements were maintained at 77 K with a liquid nitrogen bath.

Computational description

Geometry optimizations were performed with Gaussian 03[19] using the B3LYP method[20] with the 6-31G(d) basis set,[21] followed by single point energy calculation at the 6-311++G(2df, 2p) level, in a density functional theory (DFT) type calculation. The initial atomic coordinates for both the molecules were taken from the crystal structures.

Results and discussion

Design of Ligand

Zwitterionic complexes become interesting subject of matter, as it can act as ionic liquid precursors or ionic liquids for potential applications as cleaner and green and environmentally friendly reaction media in organic processes.[22] The ligand H_3TTTPC is a zwitterionic flexible ligand. Moreover, in the previous study it was shown that the ligand preferred *cis* conformation,[23] not only with metal binding state (in MOF) but also the ligand alone. This conformation is less stable than its *trans* as in the *cis* conformation all the three phenyl rings are in same side of the central aromatic ring and make steric hindrance among themselves (Figure 3b). Since former rings are connected with later *via* methylene group (─CH_2), there is a chance to rotate and get stable conformation. By getting inspiration from this fact, we chose lanthanides for this ligand to change the conformation as these metals has tendency to form large coordination number, which may lead the ligand to adopt trans conformation for reducing steric hindrance.

Syntheses and crystal structures

The crystals synthesized by microwave heating (when the experiment was performed for 30 min.) have similar sizes and shapes to those obtained by conventional solvothermal method (Fig. S9), while the same was performed for 5 min, only microcrystalline solids were obtained which is proved in SEM images (Figure S13). But the purity of these solids was examined by PXRD (Figure S3), where the patterns are perfectly matching with simulated data.

The single-crystal X-ray diffraction studies performed on **1−9** reveal that all nine MOFs are 3D frameworks, crystallizing in the triclinic *P*-1 space group. Since these are isostructural, herein, only the structure of **2** will be described in detail as a representative. Each asymmetric unit of **2** contains one

crystallographically independent cerium ion, one TTTPC[3-] ligand, two coordinated water molecules as ligand, two nitrate and one chloride anion. In this structure, the conformation of
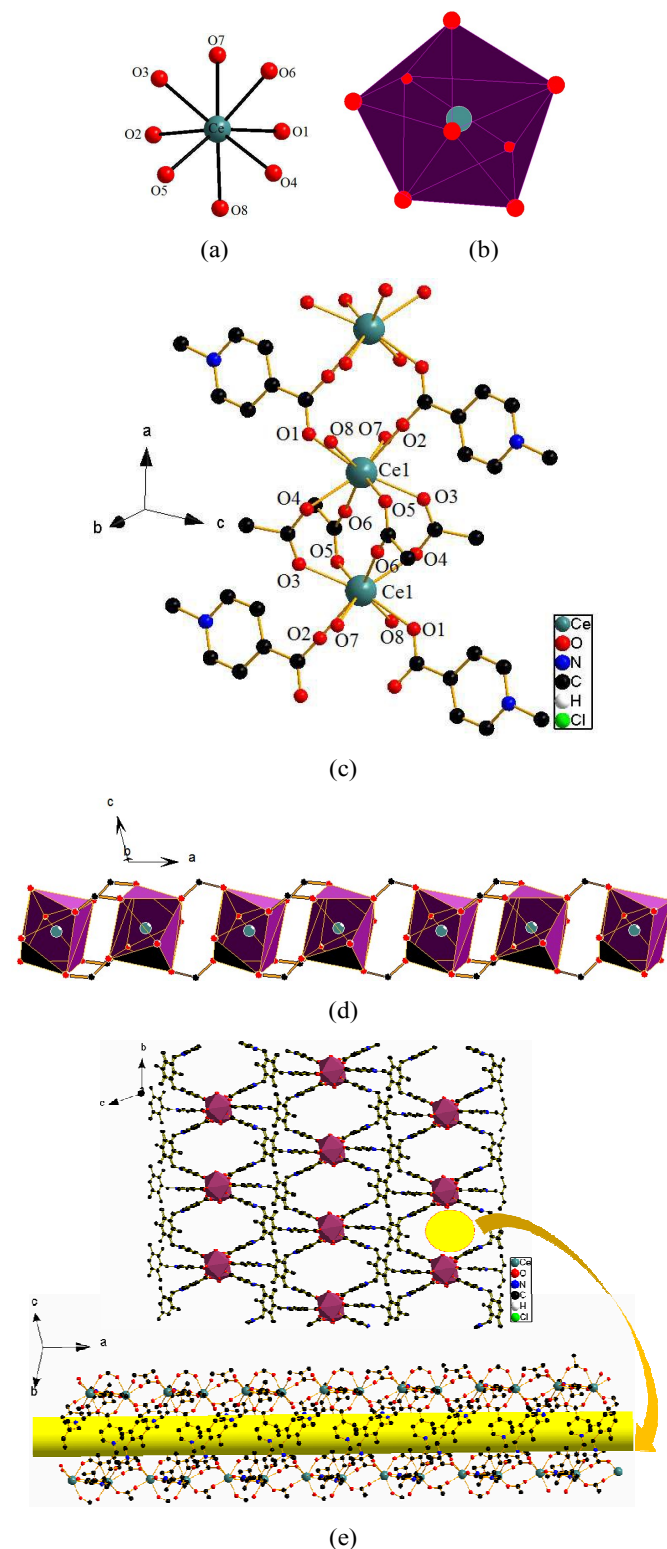
Figure 1. (a) Coordination environment of central metal ion. (b) Dodecahedral geometry of the central metal ion. (c) Two adjacent Ce^{3+} ions are bridged by four carboxylate groups from four TTTPC ligands to yield paddel-whele structure. (d) Inorganic building block growing along *a*-axis. (e) 3-D packing view of Ln-MOF

along *a*-axis, where narrow chanels (indicated by yellow cylinder) are formed along *a*-axis.

---

ligand is like chair *i.e.*, "*anti*" (Here we used two terms "*syn*" and "*anti*" refer to all the three carboxylic group containing phenyl ring are in same side and both side of the central phenyl ring of ligand, respectively (Figure 3a and 3b)) which is more stable form than "*syn*" conformation. Theoretical study also supports this phenomenon. The angles between terminal and central phenyl rings are 111.14˚, 112.17˚ and 116.03˚ (for "*syn*" conformation) and 112.18˚, 113.54˚ and 112.52˚ (for "*anti*" conformation). The coordination number of central metal ion is eight (Figure 1a). Each eight coordinated Ce^{3+} centers are in dodecahedral geometries (Figure 1b). The inorganic building block are formed by alternating four and two carboxilic acid group and grown along the *a*-axis (Figure 1d). The coordination of carboxylate ions to metal ions can be categorized in three types depending on the C−O···M angle.[24] In this structure two adjacent Ce^{3+} ions are bridged by four carboxylate groups to yield paddel-wheel structure (Figure 1c). The O−Ln (here Ln represents MOF forming lanthanides) bond lengths are in the range of 2.275(4)−2.579(5) Å, (Table S1−S9 of the Supporting Information) all of which are similar to those of other reported Ln-MOFs.[9,25] As shown in Figure 1c, two eight coordinated Ce^{3+} ions are coupled in pairs by four TTTPC carboxylate groups and four H_2O to form a secondary building unit (SBU) $\{Ce_2(COO)_4(H_2O)_4\}$, whereas TTTPC acts as a hexadentate ligand. The two paddle-wheel units are connected by carboxylate group of two ligands to form a narrow 1D channel indicating by yellow cylinder along the *a*-axis forming a 3D structure Figure 1e. PLATON[16] calculations show that the guest accessible volume (2108.8 Å^3 and 2068.9 Å^3 per unit cell) comprises 28.5 % and 27.3 % for **1** and **8**, of the unit cell volume, respectively.
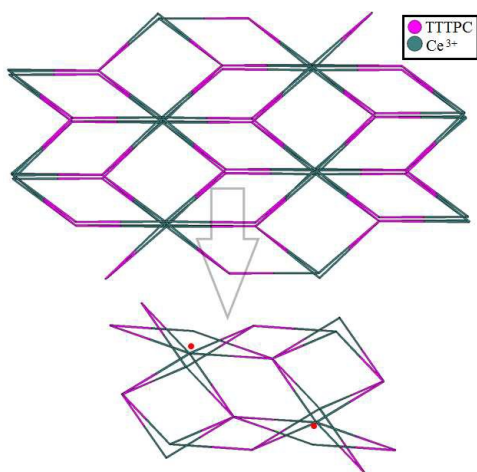
Figure 2. Topological representation of the uninodal frameworks of [Ln(TTTPC)(O)$_2$], where TTTPC is hexadented ligand and Ln, lanthanum ion. For clarity a portion is depicted below, where it is clearly visualized the hexadented ligand (pink colour) and the metal center (teal colour, marked by red point) are in six coordination environment. (the other two coordination site occupied by two water molecules, not considered for topology calculation)

To improve our understanding of the framework topology, the dinuclear Ce^{3+} (since all the MOFs are isostructural, the topology was determined for Ce^{3+} as a representative) units that connect with six organic ligands can be simplified into trigonal prismatic 6-connected nodes, and the organic ligand serves also as 6-connected node (Figure 1c); therefore, these two kinds of nodes alter the connection and then present an unprecedented 6-connected uninodal net with the point (Schläfli) symbol $\{4^{11}.6^{4}\}$ having vertex symbol of [4.4.4.4.4.4.4.4.4.4.4.4(3).4(3).6(2).6(2).6(2).6(2)] (Figure 2). To the best of our knowledge, this topology (sqc 885) is new.[26]

Thermal stability analysis

Thermal gravimetric analyses (TGA) of all the MOF's were performed on a NETZSCH STA 449C instrument. Since these compounds are isostructural, all of these MOFs material show similar thermal stability. The first weight loss at 25 °C to ~131 °C may be due to loss of isolated water molecule, second weight loss at 188 °C may be due to co-ordinated water molecule and third weight loss may corresponds to the decomposition of the moity (Figure S6). These MOF's are stable at least up to 131 °C. The frameworks start to burn off with the loss of TTTPC^{3-} ligand above 300 °C.

Density functional theory calculation

The conformation versatility is common phenomena for flexible ligand,[27] but the ligand H$_3$TTTPC is not known to show any such phenomena in its metal complex or metal organic framework, in the literature reported thus far. In the previous report it was mentioned that the ligand was adopted only bowl (*syn*) conformation in all the structures and all the metal coordination polymer were made by transition metals (Cu^{2+}, Zn^{2+} and Cd^{2+}).[23] In our curiosity, to change the conformation of this ligand we used lanthanides, since it contains a large coordination centre. Successfully we are able to change the conformation. To rationalize the different conformation in H$_3$TTTPC, we performed DFT calculations using Gaussian software. The calculations were performed on the free TTTPC^{3-} for estimating the relative energy differences of the two possible conformations. In both the cases, the molecules were taken from corresponding crystal structures and performed geometry optimization, followed by the single point energy calculations. The calculations reveal that the "*anti*" conformation is more stable than the "*syn*" conformation by 2.41 kcal/mol per molecule. The reduced stability of the free "*syn*" TTTPC^{3-} is attributable to the distress caused by the steric hindrance among three phenyl rings. But, since the size of transition metals are small and less tendency to make large coordination number it can compensate the steric repulsion by favoring "*syn*" conformation. However, in the case of lanthanides, due to large coordination capability, favor only "*anti*" conformation to minimize steric repulsion. The preferable repulsions are between −CH$_3$ groups of central phenyl ring and also between −CH$_3$ and −CH$_2$ groups (indicated by pink colour) (Figure 3c).
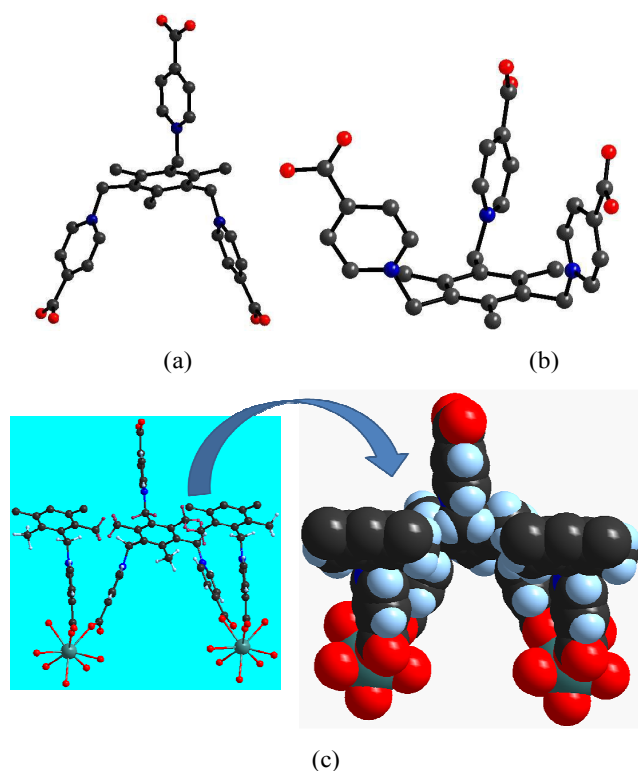
Figure 3. Presentation of two conformations of TTTPC^{3-}. (a) "*anti*" conformation and (b) "*syn*" conformation. (c) Steric repulsion between —CH$_3$ groups of central phenyl ring and also between —CH$_3$ and —CH$_2$ groups (indicated by pink colour).

Adsorption study

Since all the Ln-MOFs are isostructural frameworks (1−9), the atomic number of lanthanide cations increasing from La to Lu, the molecular mass becomes larger and therefore, it is reasonable to expect that the gravimetric adsorption capacities tend to gradually decrease from compound **1** (La) to **9** (Yb). So, as a representative, only the sorption properties of **1** (smallest formula weight) and **8** (medium formula weight) will be studied in detail. Before the measurements, the samples of **1** and **8** were soaked in methanol and activated by supercritical carbon dioxide (SCD) method (Experimental Section). The complete elimination of the H$_2$O molecules in the desolvated samples were confirmed by the IR spectra (Figure S1). The PXRD patterns for desolvated samples are similar to that of the as synthesized samples, indicating that the departure of the guest molecules does not lead to an obvious phase transformation (Figure S5).

The permanent porosity of microporous Ln-MOFs is confirmed by their N$_2$ sorption isotherms at 77 K. As shown in Figure 3, N$_2$ adsorption isotherms of the two fully activated MOFs reveal typical type-II isotherm, which represents unrestricted monolayer-multilayer adsorption. Reduction of the pressure after saturation of the sample results in a non-closing hysteresis in the desorption process, corresponding to the H$_4$ type hysteresis loops (Figure. S10), which is often associated with narrow slit-like pores.[28] This phenomenon is probably due to relatively small intersecting channels compared with the inner

cavities of cages. Calculated from the nitrogen adsorption data, the Langmuir surface area of **1** and **8** are 104 m^2 g^{-1} 57 m^2 g^{-1} (54 m^2 g^{-1} and 34 m^2 g^{-1} BET) respectively. The former is smaller than the Connolly surface area estimated based on the crystal structure (138 m^2 g^{-1} and 123 m^2 g^{-1} using a spherical probe of 1.8 Å in diameter). The discrepancy indicates the incomplete removal of guest molecules or structural deformation during the thermal activation of **1** and **8**, which is often observed in MOFs.[29] The approx diameter of pore of the 1D narrow channel (Figure 1e, indicated by yellow cylinder) is 7.5 Å. H$_2$ adsorption measurements were performed at 77 K and 273 K to investigate the H$_2$ uptake capacities (Figure 4). The H$_2$ uptake of **1** and **8**, at 77 K and 1 atm is 76 mL g^{-1} or 0.67 wt% and 55 mL g^{-1} or 0.49 wt%. The H$_2$ uptake of **1** is comparable to our previous reported MOF.[9]
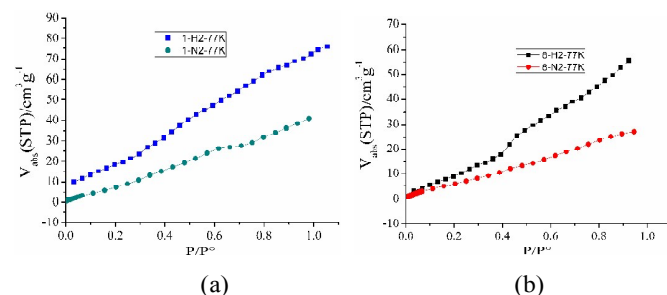
**Figure 4.** Low-pressure N$_2$ and H$_2$ sorption isotherms for 1 (a) and 3 (b) at 77 K.

Photolminescence property

The excitation spectra of Ln^{3+} carboxylates (Figure S11) exhibits a broad band between 250 and 350nm (λmax = 280 nm), which is attributable to the $\pi-\pi*$ transition of the aromatic carboxylate ligand. Apart from this broad absorption band, a series of sharp lines that are assignable to *f–f* transitions are also observed in the excitation spectra of the complexes. The latter transitions, $^5L_6\leftarrow{}^7F_0$ for Eu^{3+} and $^5L_{10}$, $^5G_6$, $^5G_3\leftarrow{}^7L_6$ for Tb^{3+} are weaker than the bands due to the organic ligands, pointing to the fact that the aromatic carboxylate ligand can act an efficient antenna molecule for Eu^{3+} and Tb^{3+} ions.

When excited at the ligand centered band at 280 nm, both the Ln^{3+} MOFs (Ln =Eu, Tb) shows the characteristic *f–f* transitions in the visible region. Figure 5a presents the corrected emission spectrum of Eu^{3+} complex in the solid state. The emission spectrum composed of five distinct transitions due to the radiative deactivation of the first excited state $^5D_0$ to the ground state manifold $^7F_{0-6}$ of Eu^{3+}. The emission spectrum shows only one peak for the $^5D_0\rightarrow{}^7F_0$ transition at 578 nm, indicating the presence of a single chemical environment. The highest intensity of emission at 612 nm in the red region is attributed to $^5D_0\rightarrow{}^7F_2$ transition. The emission in the orange region, at 592 nm corresponds to the $^5D_0\rightarrow7F_1$ transition, and emission bands 648 nm and at 698 nm are corresponds to $^5D_0\rightarrow{}^7F_3$, $^5D_0\rightarrow{}^7F_4$ transitions, respectively. The spectrum is dominated by the $^5D_0\rightarrow{}^7F_1$ (magnetic dipole transition) and hyper sensitive $^5D_0\rightarrow{}^7F_2$ (electric dipole transitions) are responsible for the intense orange-red emission color of the

Eu^{3+} MOF. The higher relative intensity of $^5D_0 \rightarrow ^7F_1$ peak in the present system gave strong indication for the existence of a Eu^{3+} in centrosymmetric field, which is inconsistence with the symmetry (P-1) obtained from the single crystal data analysis. On the other hand the Tb^{3+} MOF shows brilliant green emission under U-V irradiation. The solid state emission spectrum (Figure 5b) obtained by exciting the Tb^{3+} MOF at 280 nm shows the four expected peaks due to the transitions of $^5D_4 \rightarrow ^7F_{6-0}$ with high intensity. All these transitions are well resolved and can be assigned to the transitions $^5D_4 \rightarrow ^7F_6$ (488 nm), $^5D_4 \rightarrow ^7F_5$ (543 nm), $^5D_4 \rightarrow ^7F_4$ (586 nm), $^5D_4 \rightarrow ^7F_3$ (618 nm), and $^5D_4 \rightarrow ^7F_{2-0}$ (645-675 nm), respectively. The higher relative intensity of $^5D_4 \rightarrow ^7F_6$ peak in the present system also gave strong indication for the existence of a Tb^{3+} in centrosymmetric field, which is again inconsistence with the symmetry (P-1) obtained from the single crystal data analysis.
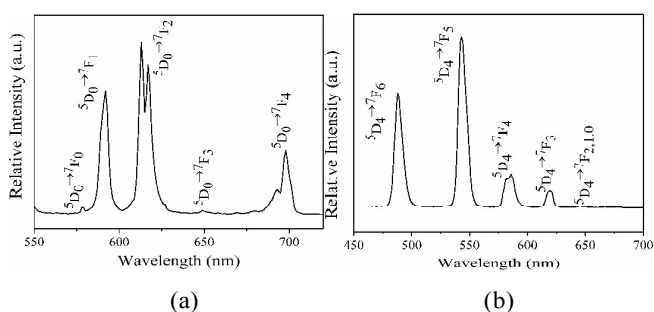
Figure 5. Corrected emission spectra for **5** and **6** in the solid state at 298 K (λex = 275 nm).

Conclusions

In summary, we have successfully synthesized a laboratory large scale (2 g) of a series of Ln-MOFs formulated as [Ln(TTTPC)(NO2)2(Cl)]·(H2O)10 {Ln = La (**1**), Ce (**2**), Pr (**3**), Nd (**4**), Eu (**5**), Tb (**6**), Dy (**7**), Ho (**8**), Yb (**9**); H3TTTPC = 1,1',1"-tris(2,4,6-trimethylbenzene-1,3,5-triyl)-tris(methylene)-tris(pyridine-4-carboxylic acid)} with high purity under microwave conditions rapidly and efficiently, and their photoluminescence spectra and gas adsorption properties were also investigated. All the structures adopts "anti" conformation which is stable form, predicted from theoretical calculation and exhibiting a new uninodal structural topology. Compounds **5** and **6** show efficient antenna effect and have shown the data is inconsistence with the symmetry (P-1) obtained from the single crystal data analysis. Compounds **1** and **8** retain structural integrity and permanent microporosity after guest removal, with moderate capability of gas adsorption for hydrogen. The present work may open new perspectives in this field of research based on the simple idea of conformation change of flexible ligand using lanthanides and microwave-assisted scale up synthesis of Ln-MOF in laboratory large scale with high purity using green solvent (water and ethanol) which are environment friendly.

Acknowledgements

Notes and references

State Key Laboratory of Structural Chemistry, Fujian Institute of Research on the Structure of Matter, Chinese Academy of Sciences, Fujian, Fuzhou 350002, P. R. China. *E-mail: rcao@fjirsm.ac.cn. Phone: +86-591-83725186. Fax: +86-591-83796710.

1   (a) M. O'Keeffe, O. M. Yaghi, *Chem. Rev.*, 2012, **112**, 675. (b) H. Deng, S. Grunder, K. E. Cordova, C. Valente, H. Furukawa, M. Hmadeh, F. Gándara, A. C. Whalley, Z. Liu, S. Asahina, H. Kazumori, M. O'Keeffe, O. Terasaki, J. F. Stoddart, O. M. Yaghi, *Science*, 2012, **336**, 1018. (c) Y. Cui, Y. Yue, G. Qian, B. Chen, *Chem. Rev.*, 2012, **112**, 1126. (d) M. H. Alkordi, J. A. Brant, L. Wojtas, V. C. Kravtsov, A. J. Cairns, M. Eddaoudi, *J. Am. Chem. Soc.*, 2009, **131**, 17753. (e) F. Nouar, J. F. Eubank, T. Bousquet, L. Wojtas, M. J. Zaworotko, M. Eddaoudi, *J. Am. Chem. Soc.*, 2008, **130**, 1833. (f) M. Eddaoudi, J. Kim, N. Rosi, D. Vodak, J. Wachter, M. O'Keeffe, O. M. Yaghi, *Science*, 2002, **295**, 469.

2   (a) J.-P. Lang, Q.-F. Xu, R.-X. Yuan, and B. F. Abrahams, *Angew. Chem. Int. Ed.*, 2004, **43**, 4741. (b) R. Babarao, R. Custelcean, B. P. Hay, D. E. Jiang, *Cryst. Growth Des.*, 2012, 12, 5349. (c) D. Dubbeldam, C. J. Galvin, K. S. Walton, D. E. Ellis, R. Q. Snurr, *J. Am. Chem. Soc.*, 2008, **130**, 10884. (d) D. Feng, Z. Y. Gu, J. R. Li, H. L. Jiang, Z. Wei, H. C. Zhou, *Angew. Chem. Int. Ed.*, 2012, **51**, 10307. (e) D. W. Fu, W. Zhang, H. L. Cai, Y. Zhang, J. Z. Ge, R.-G. Xiong, S. D. Huang, *J. Am. Chem. Soc.*, 2011, **133**, 12780. (f) Z. R. Herm, J. A. Swisher, B. Smit, R. Krishna, J. R. Long, *J. Am. Chem. Soc.*, 2011, **133**, 5664. (g) D. Liu, J.-P. Lang, and B. F. Abrahams, *J. Am. Chem. Soc.*, 2011, **133**, 11042. (h) J. R. Li, J. Sculley, H. C. *Chem. Rev.*, 2012, **112**, 869. (i) M. P. Suh, H. J. Park, T. K. Prasad, D. W. Lim, *Chem. Rev.*, 2012, **112**, 782. (j) K. Sumida, D. L. Rogow, J. A. Mason, T. M. McDonald, E. D. Bloch, Z. R. Herm, T. H. Bae, J. R. Long, *Chem. Rev.*, 2012, **112**, 724.

3   (a) Y. Yu, J. P. Ma, Y. B. Dong, *CrystEngComm* 2012, **14**, 7157. (b) T. Devic, V. Wagner, N. Guillou, A. Vimont, M. Haouas, M. Pascolini, C. Serre, J. Marrot, M. Daturi, F. Taulelle, G. Férey, *Micropor. Mesopor. Mat.*, 2011, **140**, 25. (c) D. T. de Lill, A. de Bettencourt-Dias, C. L. Cahill, *Inorg. Chem.*, 2007, **46**, 3960.

4   J. Rocha, L. D. Carlos, F. A. A. Paz, D. Ananias, *Chem. Soc. Rev.*, 2011, **40**, 926.

5   A. de la Hoz, A. Diaz-Ortiz, A. Moreno, *Chem. Soc. Rev.*, 2005, **34**, 164.

6   Y. Y. Hu, C. Liu, Y. H. Zhang, N. Ren, Y. Tang, *Micropor. Mesopor. Mat.*, 2009, **119**, 306.

7   (a) J.-P. Lang, K. Tatsumi, H. Kawaguchi, J. Lu, P. Ge, W. Ji, and S. Shi, *Inorg. Chem.*, 1996, **35**, 7924. (b) S.-H. Zhang, M.-F. Tang, C.-M. Ge, *Z. Anorg. Allg. Chem.*, 2009, **635**, 1442. (c) S.-H. Zhang, Y. Song, H. Liang, M.-H. Zeng, *CrystEngComm*, 2009, **11**, 865. (d) C. J. Milios, A. Vinslava, A. G. Whittaker, S. Parsons, W. Wernsdorfer, G. Christou, S. P. Perlepes, E. K. Brechin, *Inorg. Chem.*, 2006, **45**, 5272. (e) I. A. Gass, C. J. Milios, A. G. Whittaker, F. P. A. Fabiani, S. Parsons, M. Murrie, S. P. Perlepes, E. K. Brechin, *Inorg. Chem.*, 2006, **45**, 5281.

8   (a) J. Klinowski, F. A. Almeida Paz, P. Silva, J. Rocha, *Dalton Trans.*, 2011, 40, 321. (b) Z. H. Xiang, D. P. Cao, X. H. Shao, W. C. Wang, J. W. Zhang, W. Z. Wu, *Chem. Eng. Sci.*, 2010, **65**, 3140. (c) Y. K. Seo, G. Hundal, I. T. Jang, Y. K. Hwang, C. H. Jun, J. S. Chang, *Micropor. Mesopor. Mat.*, 2009, **119**, 331. (d) S. H. Jhung, J. H. Lee, J. W. Yoon, C. Serre, G. Ferey,; J. S. Chang, *Adv. Mater.*, 2007, **19**, 121.

9   Z.-J. Lin, Z. Yang, T.-F. Liu, Y.-B. Huang, and R. Cao, *Inorg. Chem.*, 2012, **51**, 1813.

10   a) P. Silva, A. A. Valente, J. Rocha, F. A. A. Paz, *Cryst. Growth Des.*, 2010, **10**, 2025. (b) W. L. Liu, L. H. Ye, X. F. Liu, L. M. Yuan, X. L. Lu, J. X. Jiang, *Inorg. Chem. Commun.*, 2008, **11**, 1250. (c) P. Amo-Ochoa, G. Givaja, P. J. S. Miguel, O. Castillo, F. Zamora, *Inorg. Chem. Commun.*, 2007, **10**, 921. (d) Z. Lin, D. S. Wragg, R. E. Morris, *Chem. Commun.*, 2006, **42**, 2021. (e) S. H. Jhung, J.-H. Lee, P. M. Forster, G. Férey, A. K. Cheetham, J.-S. Chang, *Chem.Eur. J.*, 2006, **12**, 7899.

11   W. Lu, Z. Wei, Z.-Y. Gu, T.-F. Liu, J. Park, J. Park, J. Tian, M. Zhang, Q. Zhang, T. Gentle III, M. Bosch and H.-C. Zhou, *Chem. Soc. Rev.*, 2014, **43**, 5561.

12   Z.-J. Lin, J. Lü, M. Hong and R. Cao, *Chem. Soc. Rev.*, 2014, **43**, 5867.

13   (a) C. A. Fernandez, P. K. Thallapally, R. K.Motkuri, S. K. Nune, J. C. Sumrak, J. Tian and J. Liu, *Cryst. Growth Des.*, 2010, **10**, 1037; (b) T.-F. Liu, J. Lu and R. Cao, *CrystEngComm*, 2010, **12**, 660; (c) F. C. Pigge, *CrystEngComm*, 2011, **13**, 1733.

14   G. M. Sheldrick, *SHELXS-97*, *Program for Crystal Structure Solution and Refinement*; University of Göttingen: Gottingen, Germany, 1997.

15   SHELXL, G.M. Sheldrick, *Acta Cryst.*, 2008, **A64**, 112.

16   (a) A. L. Spek, *J. Appl. Crystallogr.*, 2003, **36**, 7. (b) P. v.d. Sluis and A. L. Spek, *Acta Crystallogr., Sect. A*, 1990, **46**, 194.

17   (a) Q. R. Fang, G. S. Zhu, M. Xue, J. Y. Sun, F. X. Sun, S. L., *Inorg. Chem.*, 2006, **45**, 3582; (b) J. H. He, Y. T. Zhang, Q. H. Pan, J. H. Yu, H. Ding, R. R. Xu, *Micropor. Mesopor. Mat.*, 2006, **90**, 145 (c) S. Zheng, T. Wu, J. Zhang, M. Chow, R. A. Nieto, P. Feng, X. Bu, *Angew. Chem. Int. Ed.*, 2010, **49**, 5362. (d) X. -R. Hao, X. -L. Wang, K. -Z. Shao, G. -S. Yang, Z. -M.

Su, G. Yuan, *CrystEngComm.*, 2012, **14**, 5596 (e) H. -L. Li, M. Eddaoudi, M. O'Keeffe, O. M. Yaghi, *Nature*, 1999, **402**, 276.

18   (a) A. P. Nelson, O. K. Farha, K. L. Mulfort, J. T. Hupp, *J. Am. Chem. Soc.*, 2009, **131**, 458. (b) O. K. Farha, J. T. Hupp, *Acc. Chem. Res.*, 2010, **43**, 1166. (c) A. I. Cooper, M. J. Rosseinsky, *Nat. Chem.*, 2009, **1**, 26. (d) D. Han, F. L. Jiang, M. Y. Wu, L. Chen, Q. H. Chen, M.-C. Hong, *Chem. Commun.*, 2011, **47**, 9861.

19   M. J. Frisch, G. W. Trucks, H. B. Schlegel, G. E. Scuseria, M. A. Robb, J. R. Cheeseman, J. A. Montgomery, T. Vreven, K. N. Kudin, J. C. Burant, J. M. Millam, S. S. Iyengar, J. Tomasi, V. Barone, B. Mennucci, M. Cossi, G. Scalmani, N. Rega, G. A. Petersson, H. Nakatsuji, M. Hada, M. Ehara, K. Toyota, R. Fukuda, J. Hasegawa, M. Ishida, T. Nakajima, Y. Honda, O. Kitao, H. Nakai, M. Klene, X. Li, J. E. Knox, H. P. Hratchian, J. B. Cross, V. Bakken, C. Adamo, J. Jaramillo, R. Gomperts, R. E. Stratmann, O. Yazyev, A. J. Austin, R. Cammi, C. Pomelli, J. W. Ochterski, P. Y. Ayala, K. Morokuma, G. A. Voth, P. Salvador, J. J. Dannenberg, V. G. Zakrzewski, S. Dapprich, A. D. Daniels, M. C. Strain, O. Farkas, D. K. Malick, A. D. Rabuck, K. Raghavachari, J. B. Foresman, J. V. Ortiz, Q. Cui, A. G. Baboul, S. Clifford, J. Cioslowski, B. Stefanov, G. Liu, A. Liashenko, P. Piskorz, I. Komaromi, R. L. Martin, D. J. Fox, T. Keith, M. A. Al-Laham, C. Y. Peng, A. Nanayakkara, M. Challacombe, P. M. W. Gill, B. Johnson, W. Chen, M. W. Wong, C. Gonzalez, J. A. Pople, *Gaussian 03*, revision E. 01, Wallingford CT: Gaussian, Inc. 2004.

20   (a) A. D. Becke, *J. Chem. Phys.*, 1993, **98**, 5648. (b) C. Lee, W. Yang, R. G. Parr, *Phys. Rev. B*, 1988, **37**, 785.

21   (a) W. J. Hehre, R. Ditchfield, J. A. Pople, *J. Chem. Phys.*, 1972, **56**, 2257. (b) P. C. Hariharan, J. A. Pople, *Theor. Chim. Acta*, 1973, **28**, 213.

22   (a) T. Welton, *Chem. Rev.*, 1999, **99**, 2071. (b) P. Wasserscheid, W. Keim, *Angew. Chem., Int. Ed.*, 2000, **39**, 3772. (c) R. Sheldon, *Chem. Commun.*, 2001, 2399. (d) J. Dupont, R. F. de Souza, P. A. Z. Suarez, *Chem. Rev.*, 2002, **102**, 3667. (e) J. Huang, T. Jiang, H. Gao, B. Han, Z. Liu, W. Wu, Y. Chang, G. Zhao, *Angew. Chem., Int. Ed.*, 2004, **43**, 1397. (f) W. Miao, T. H. Chan, *Acc. Chem. Res.*, 2006, **39**, 897.

23   G.-Q. Kong and C.-D. Wu, *Cryst. Growth Des.*, 2010, **10**, 4590.

24   C. J. Carrell, H. L. Carrell, J. Erlebacher, J. P. Glusker, *J. Am. Chem. Soc.*, 1988, **110**, 8651.

25   (a) J. Zhang, B. Zheng, T. Zhao, G. Li, Q. Huo and Y. Liu, *Cryst. Growth Des.*, 2014, **14**, 2394. (b) S. Chen, R.-Q. Fan, C.-F. Sun, P. Wang, Y.-L. Yang, Q. Su and Y. Mu, *Cryst. Growth Des.,* 2012, **12**, 1337.

26   V. A. Blatov, A. P. Shevchenko, *TOPOS*, *Version 4.0 Professional (beta evaluation)*; Samara State University: Samara, Russia, 2006 V. A. Blatov, A. P. Shevchenko, V. N. Serezhkin, *J. Appl. Crystallogr.* 2000, **33**, 1193.

27   (a) M. R. Kishan, J. Tian, P. K. Thallapally, C. A. Fernandez, S. J. Dalgarno, J. E. Warren, B. P. McGrail, J. L. Atwood, *Chem. Commun.*, 2010, **46**, 538. (b) J. Tian, R. K. Motkuri, P.

K. Thallapally, B. P. McGrail, *Cryst. Growth Des.*, 2010, **10**, 5327.

28   (a) K. S. W. Sing, D. H. Everett, R. A. W. Haul, L. Moscou, R. A. Pierotti, J. Rouquerol and T. Siemieniewska, *Pure Appl. Chem.*, 1985, **57**, 603. (b) D. Tanaka, A. Henke, K. Albrecht, M. Moeller, K. Nakagawa, S. Kitagawa and J. Groll, *Nat. Chem.*, 2010, **2**, 410.

29   A. P. Nelson, O. K. Farha, K. L. Mulfort and J. T. Hupp, *J. Am. Chem. Soc.*, 2009, **131**, 458.

Dalton Transactions Accepted Manuscript

TOC Graphics
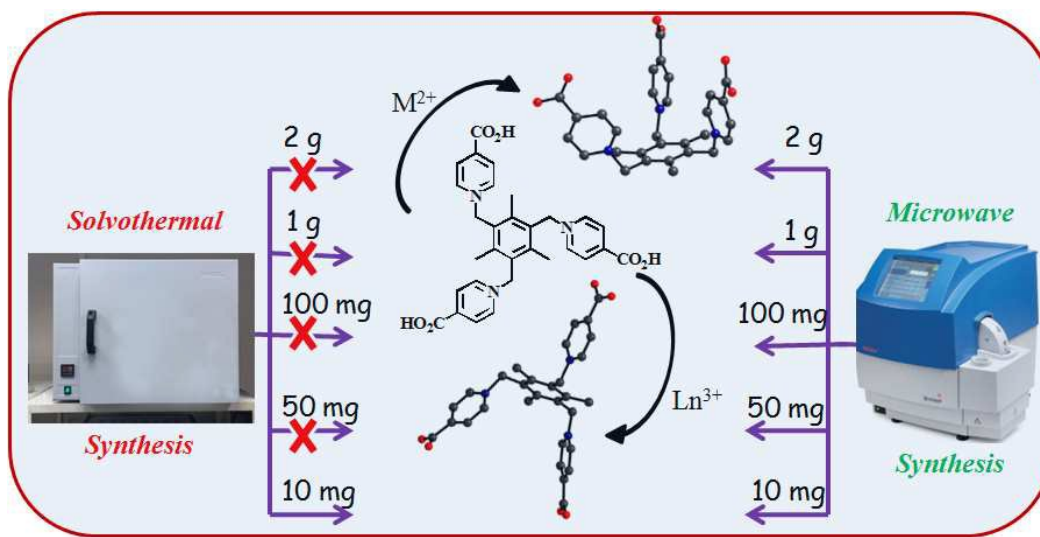
We have prepared 2g laboratory scale Ln-MOF with high purity using microwave and successfully change the conformation of flexible ligand using Ln, where Ln adopts only preferred (energetically stable) conformation from green solvent (water and ethanol). (Ln denotes lanthanide)